Confocal Microscopy Imaging of NR2B-Containing NMDA Receptors Based on Fluorescent Ifenprodil-Like Conjugates

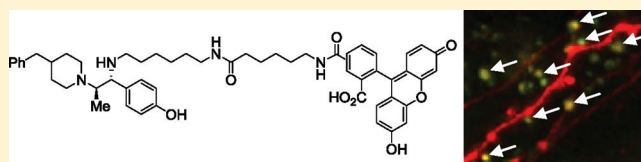Patrice Marchand,[†,‡] Javier Becerril-Ortega,[‡] Laetitia Mony,[§] Cédric Bouteiller,[†,‡] Pierre Paoletti,[§] Olivier Nicole,[‡] Louisa Barré,[†,‡] Alain Buisson,[‡] and Cécile Perrio*[,†,‡]

[†]CEA/DSV/I2BM, GDM-TEP, [‡]CI-NAPS, CNRS UMR6232, Université de Caen - Basse Normandie, Cyceron, Boulevard Henri Becquerel, 14074 Caen Cedex, France

[§]Institut de Biologie, CNRS UMR8197, INSERM U1024, Ecole Normale Supérieure, 46 rue d'Ulm, 75005 Paris, France

Ⓢ *Supporting Information*

ABSTRACT: We describe the synthesis and pharmacological characterization of a first generation of ifenprodil conjugates **4−7** as fluorescent probes for the confocal microscopy imaging of the NR2B-containing NMDA receptor. The fluorescein conjugate **6** displayed a moderate affinity for NMDAR but a high selectivity for the NR2B subunit and its NTD. Fluorescence imaging of DS-red labeled cortical neurons showed an exact colocalization of the probe **6** with small protrusions along the dendrites related to a specific binding on NR2B-containing NMDARs.
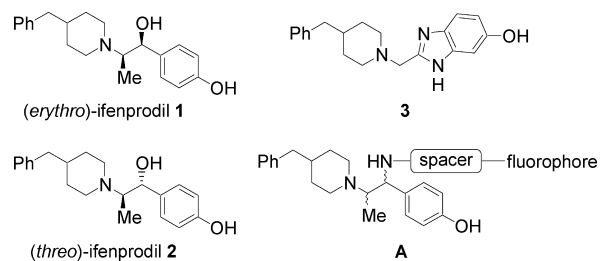
The *N*-methyl-D-aspartate receptor (NMDAR) is a ligand-gated cationic channel widely expressed in the central nervous system (CNS).[1,2] The receptor plays a critical role in excitatory neurotransmission, brain development, synaptic plasticity associated with memory formation, and central sensitization during persistent pain and excitotoxicity.[3−6] Aberrant NMDAR activity is believed to be strongly related to the neuronal loss associated with neurodegenerative disorders in the human CNS that include Alzheimer's and Parkinson's diseases. The architecture of the NMDAR has been elucidated in great detail: it is a heterotetrameric complex made up of a combination of two major subunits, termed NR1 and NR2, based on the amino acid sequence identity.[7−9] Although NR1 is encoded by a single gene, the NR2 subunit exists as four subtypes encoded by four different genes (NR2A-D), each with a distinctive spatiotemporal pattern of expression. It is clear that the pharmacological and functional properties of NMDAR are highly dependent on the NR2 isoform, of which NR2A and NR2B are the most abundant. Furthermore, it has been suggested that, within an individual neuron, synaptic NMDAR subtypes can be segregated in an input-specific manner.[10] Synaptic NMDAR activation has an antiapoptotic activity, while stimulation of extrasynaptic NMDARs elicits glutamate-induced toxicity.[11] Several studies have shown that NR2B subunits, while present with NR2A subunits at many synapses, appear preferentially enriched in extrasynaptic sites and may participate in pathological processes linked to glutamatergic overstimulation. This feature rends NR2B-selective antagonists as particularly attractive therapeutic agents for neuroprotection.[12]

In order to better clarify the physiological and pathological involvement of NMDAR in neuronal fate, we aimed to develop a fluorescent ligand specific for the NR2B subunit. This fluorescent tracer might be a useful tool: for the visualization of receptors in living neurons; for the characterization of the biophysical microenvironment of the binding site; and also for dynamic studies based on fluorescence imaging.[13] As far as we know, no such tracer has been developed. Usually, fluorescent probes are obtained by creating a covalent bond between the ligand and the fluorescent moiety. Challenges often are, first, to modify the ligand (especially when it is a nonpeptidic small organic molecule with poor functionality) in order to provide an attachment point for the fluorophore; second, to perform conjugation without significantly disturbing the natural binding function. Here, we report the synthesis, the physical characterization, and the biological evaluation of a first generation of fluorescent NR2B ligands with the general formula **A**, designed on the framework of ifenprodil (Figure 1). We also show, for the first time, that it is possible to locate NR2B-containing receptor in dendrites by confocal microscopy with such a probe.
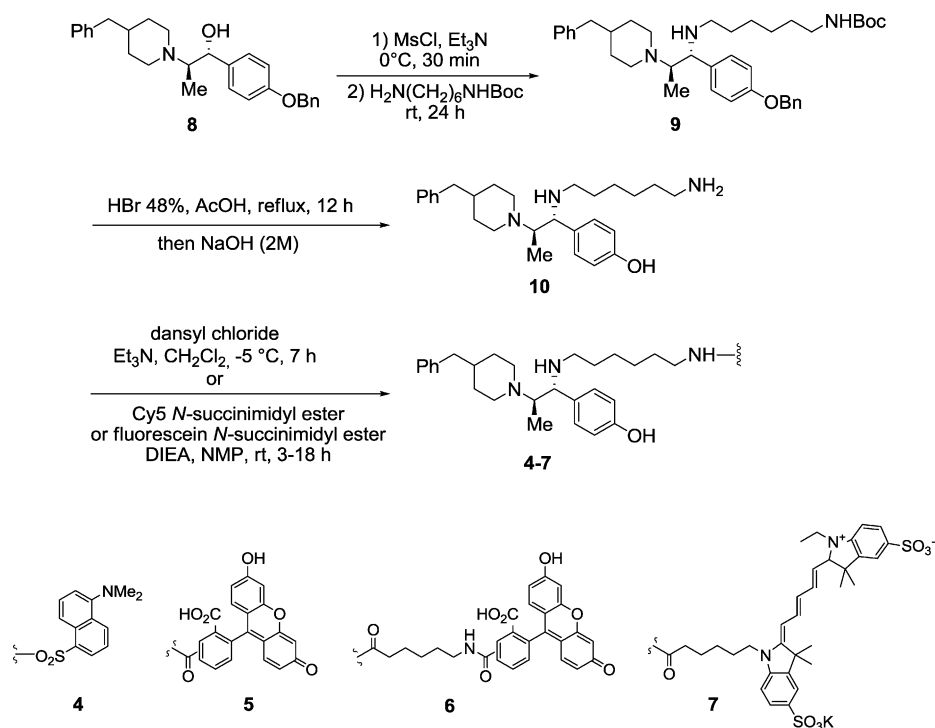

Figure 1. Selective NR1/NR2B NMDA receptor antagonists **1−3**, and general formula **A** of the target fluorescent probes.

Scheme 1. Synthesis of Fluorescent *N*-(Aminohexyl)ethylenediamine Conjugates 4−7

Ifenprodil is the lead compound of the major class of antagonists of NMDAR with marked selectivity for NR2B.[14−20] To date, it is the best characterized subtype-specific NMDA antagonist both *in vitro* and *in vivo*.[14,15,21−24] A major characteristic of ifenprodil at NMDARs is a high affinity, non-competitive, and voltage-independent inhibition of receptors endowed with the NR2B subunit. Ifenprodil contains two asymmetric centers which give rise to the two diastereoisomeric forms **1** (*erythro* or *R*S*) and **2** (*threo* or *R*R*), both of which exist as a pair of enantiomers.[24] The drug substance that has become widely used as a tool to study the expression, properties, function, and distribution of NMDAR subtypes is composed entirely of the racemic (*erythro*) diastereoisomer **1**. However, the (*threo*) racemate **2** was found to be a more potent (five times) neuroprotective agent than the (*erythro*)-diastereoisomer **1** in an *in vitro* glutamate neurotoxicity test, and the (*threo*) configuration **2** also has been suggested to be important for NMDAR selectivity.[15]

Investigations of the interaction and mechanism of action of ifenprodil on NMDARs have revealed that the ifenprodil binding site coincides with the N-terminal domain (NTD) of the NR2B subunit. The potency of ifenprodil at NR2B is due to the key structural elements that incorporate a phenolic aromatic ring connected to a second phenyl ring *via* a linker containing a tertiary basic amine.[25−29] The piperidine linker provides a scaffold to hold the two aryl rings in the optimum spatial orientation in the binding site which itself contains a lipophilic pocket that accommodates the phenyl ring, as well as a hydrophobic and hydrogen bond acceptor pocket that accepts the phenol group. The basic nitrogen atom contributes to the positioning by electrostatic interaction. By mutagenesis, it has been proposed that ifenprodil binds to the central, interlobe cleft of NR2B NTD and promotes cleft closure through a hinge-bending motion (Venus flytrap mechanism).[27] The recent characterization of binding sites by experimental and computational approaches have revealed that the phenol ring of

ifenprodil points toward the entrance of the cleft whereas the phenyl ring makes contact with the interlobe hinge.[28] On the basis of this pharmacophore/topological model, we assumed that the fluorescent moiety in derivatives **A** should not disturb the intrinsic properties of the parent ifenprodil. Hence, we selected three fluorophores, dansyl, fluorescein, and cyanine (Cy5), that possess different molecular sizes. An anchorage point for the fluorophore was provided by the secondary amine function in replacement of the benzylic hydroxyl in ifenprodil, this modification allowing the introduction of a spacer while maintaining the labile proton. Although not clearly established, the labile proton seems to be a prerequisite for selectivity based on a survey of structure−activity relationship studies.[17−21] Furthermore, it is noteworthy that ifenprodil analogues, such as the recently reported antagonist **3**, that bear a nitrogen-containing linker (i.e., an imidazole ring) instead of the hydroxypropyl moiety in ifenprodil, display an improved pharmacokinetic profile and decreased off-target activities (especially affinity for adrenergic α1 receptors and the hERG potassium channel).[30]

The synthetic route to fluorescent probes **4−7**, found to be representative of the class of compounds **A**, is depicted in Scheme 1. Racemic (*threo*)-*O*-benzyl ifenprodil **8**[15] was first converted into the ethylenediamine **9** according to a stereo-specific mesylation/amination sequence through the use of *N*-Boc-monoprotected α,ω-hexyldiamine in a 88% yield. This transformation occurred with a complete retention of configuration as a result of a mechanism with anchimeric assistance due to the *in situ* formation of an aziridinium intermediate.[31] The configuration of compound **9** was assigned by ^{1}H NMR analysis on the basis of the chemical shifts and coupling constants for the signals of protons borne by the asymmetric centers (see the Supporting Information). Acidic double deprotection of **9** led to the phenolamine **10** with a 57% yield. Conjugation of **10** with dansyl chloride, fluorescein (with or without the spacer) or cyanine Cy5 *N*-succinimidyl ester gave the probes **4−7**. These compounds were purified by
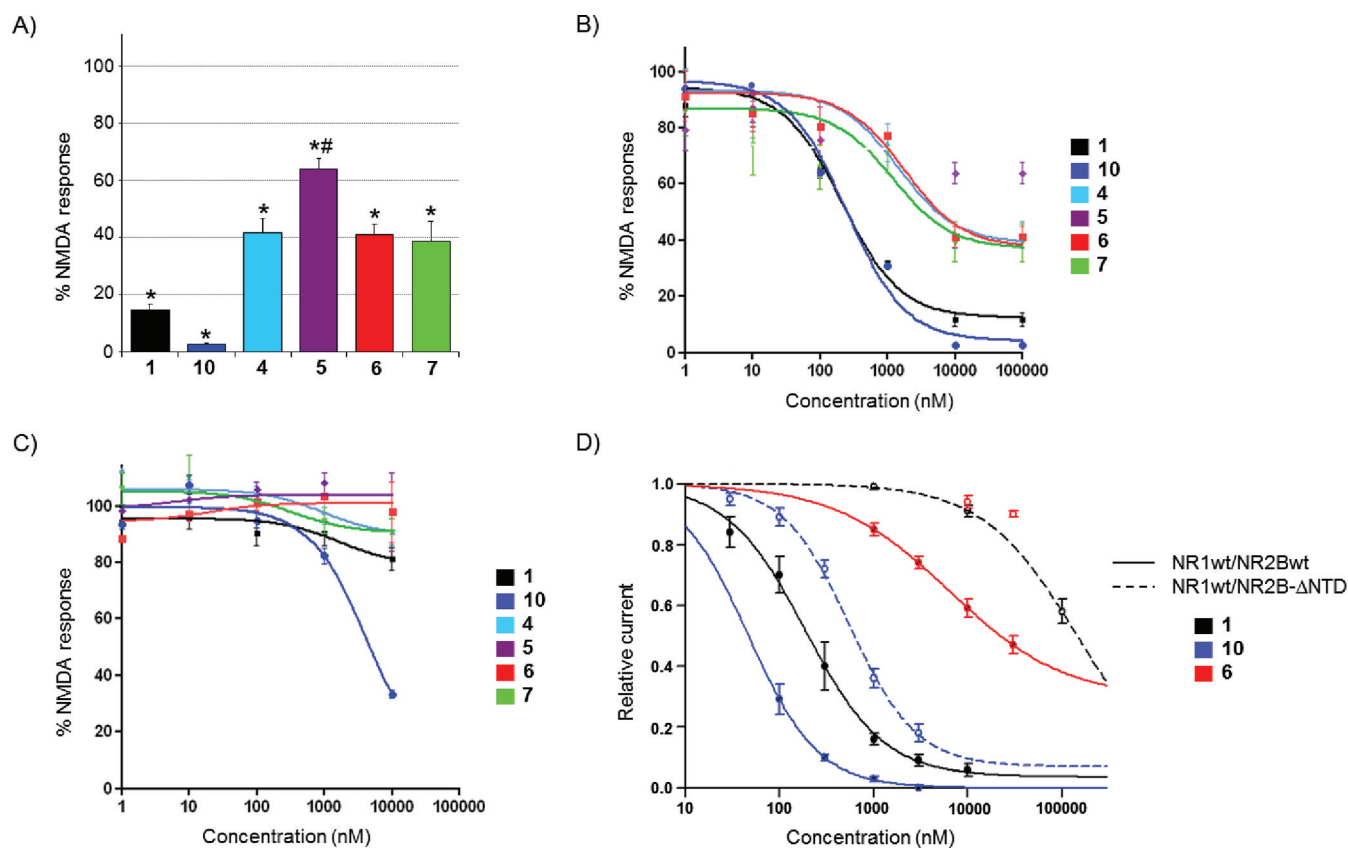
Figure 2. Evaluation of the antagonistic properties of ligands **10** and **4−7** compared to ifenprodil **1** by measurement of inhibition of NMDA-induced calcium influx (A, B, C) and NMDAR mediated currents (D). (A, B, C) Calcium imaging experiments performed by assessment of intracellular calcium increase after an acute stimulation with NMDA (100 μM) in the presence of glycine (10 μM) and ligand (n = 30 HEK cells transfected with NMDA receptor subunits from 3 independent culture dishes). Responses to ligand application were normalized to the mean response obtained by stimulation with NMDA (100 μM) in the presence of only glycine (10 μM) taken as the control experiment (100% value). (A) Histograms representing mean values of NMDA-induced calcium influx obtained with ligands (10 μM) evaluated toward NR1−1a/NR2B receptors. Statistical analysis (ANOVA) was performed on raw data [* indicates significantly different from NMDA alone (control); # indicates significantly different from **1** and NMDA alone]. (B) Dose−response curve for inhibition of NMDA-induced calcium influx through NR1−1a/NR2B receptors. (C) Dose−response curve for inhibition of NMDA-induced calcium influx through NR1−1a/NR2A receptors. (D) Electrophysiological experiments using two electrode voltage clamp (pH = 7.3; holding potential = −60 mV). NMDA currents were evoked by applying glutamate and glycine (100 μM each).

HPLC and characterized by mass spectrometry (see the Supporting Information). Spectroscopic properties were determined by UV and emission spectra measurements. Spectral properties were in accordance with the presence of dansyl, Cy5, or fluorescein [$\lambda_{ex}/\lambda_{em}$ of about 340/540 and 645/670 nm for ligands **4** and **7**, respectively, and of about 490/525 nm for both ligands **5** and **6**].

The target fluorescent conjugates **4−7** as well as the precursor **10** were evaluated as selective NR2B antagonists in a functional assay by calcium imaging (Figure 2A−C); here, we monitored intracellular calcium concentrations by videomicroscopy of HEK-293 cells transfected with the cDNA encoding either for NR1−1a and NR2B, or for NR1−1a and NR2A subunits. As NMDARs are calcium-permeable ion channels,[32] we measured calcium (Ca^{2+}) influx induced by the application of NMDA (at 100 μM for 30 s) in the presence of glycine (10 μM) and of increasing concentrations of potential antagonists. The application of NMDA induced a rapid and sustained increase in [Ca^{2+}] (determined as the 100% value), whereas the simultaneous application of NMDA and an antagonist led to a lesser increase in [Ca^{2+}]. In a first set of experiments with NR1−1a/NR2B receptor transfected cells, the compounds **4−7**

and **10** were used at 10 μM in order to perform a rapid screening (Figure 2A). The data clearly showed that the precursor **10** potently inhibited the Ca^{2+} influx with a residual NMDA response of only 3% versus 15% for ifenprodil **1**. Although moderate, the inhibition of Ca^{2+} entry by conjugates **4**, **6**, and **7** was significant (the residual responses to NMDA were approximately 40%). Ligand **5**, in contrast, showed weak effects with a residual response to NMDA superior to 60%. The pharmacological characterization of **4−7** and **10** was then pursued in a second set of experiments with either NR1−1a/NR2B or NR1−1a/NR2A receptor transfected cells by establishing the dose−response curves (Figure 2B and C). The results confirmed that precursor **10** was a potent antagonist of the NR1−1a/NR2B receptor with an IC$_{50}$ value slightly lower than that of ifenprodil **1** and that conjugates **4**, **6**, and **7** were only moderate inhibitors with IC$_{50}$ values 4- to 6-fold higher (Table 1). Thus, the chemical modification of ifenprodil **1** into ethylenediamine **10** maintained NR2B inhibition but the introduction of the fluorophore moderately decreased ligand binding. In the case of the sterically hindered cyanine and fluorescein structures, the magnitude of this decrease was minimized by increasing the spacer length (see compounds **6** and **7** versus **5** and **4**). Finally,

Table 1. Inhibition Constants IC$_{50}$ (μM, mean value $\pm$ sem) of Compounds 10 and 4−7 at NR1-1a/NR2B and NR1-1a/NR2A Receptor Subtypes Compared to Ifenprodil 1

| | calcium imaging assay | | electrophysiology | |
compound	NR2B	NR2A	NR2B	NR2B-ΔNTD
1	0.275 $\pm$ 0.034	>100	0.190 $\pm$ 0.020	145 $\pm$ 2.000
10	0.244 $\pm$ 0.036	4.440 $\pm$ 0.755	0.047 $\pm$ 0.002	0.560 $\pm$ 0.090
4	1.416 $\pm$ 0.411	>100	n.d.	n.d.
5	>10	>100	n.d.	n.d.
6	1.795 $\pm$ 0.535	>100	6.400 $\pm$ 0.300	>100
7	1.203 $\pm$ 0.630	>100	n.d.	n.d.

ligands **4**, **6**, **7**, and **10** did not display any effect on NR1−1a/NR2A receptor transfected cells (except for **10** at concentration higher than 10 μM), which rend them highly selective toward the NR1−1a/NR2B receptor (Figure 2C).

A further evaluation of precursor **10** and conjugate **6** was performed in electrophysiological studies using two-electrode voltage-clamp measurements in *Xenopus laevis* oocytes that expressed recombinant NMDARs after the coinjection of cDNAs coding for wild-type (wt) NR1−1a and either wild-type NR2B or a NTD deleted NR2B subunit (Figure 2D). NMDA currents were induced by saturating concentrations of L-glutamate and glycine (100 μM each),[9,33] and the effects of ligands **10** and **6** were assessed by measuring the change in current size induced by the application of the compound during a NMDA response.[27,28] The results confirmed that ligand **10** inhibited NR1wt/NR2Bwt receptors. Inhibition by **10** was found complete (no residual current could be measured), whereas 4% of the residual current remained with ifenprodil **1** applied at saturating concentrations. Ligand **10** also displayed an inhibitory effect on NR1wt/NR2-ΔNTD receptors with an IC$_{50}$ ~12 fold higher than that measured on the full-length receptors (Table 1). This inhibition was found to be voltage-dependent, and disappeared almost completely at depolarized potentials (data not shown). This effect probably results from an interaction of **10** with the ion channel pore as reported for polyamines such as spermine and spermidine.[34,35] This possibility could explain the low but significant inhibition of NR2A-containing receptors by compound **10** as assessed by the calcium imaging experiments (Figure 2C). The inhibition of NR2B-containing receptors by conjugate **6** was decreased when compared to precursor **10** as demonstrated by the greater IC$_{50}$ values obtained in the current assays (Table 1). Interestingly, no inhibitory effects were detected at NR1wt/NR2-ΔNTD receptors with the conjugate **6** (Figure 2D). Thus, as shown in the calcium imaging assay, the fluorophore conjugation led to a decreased affinity though to an increased selectivity. A simple explanation might be that the interaction in the channel pore fails to occur due to the lack of a single cationic site (i.e., the terminal primary amine function) in conjugate **6** as compared to precursor ligand **10**.

Confocal microscopy imaging studies were carried out by fluorescence analysis of DS-red labeled cortical neurons incubated with conjugate **6** ($\lambda_{ex}/\lambda_{em}$ = 490/525 nm). Primary neuronal cultures (at DIV 10) were transfected with the DS-red fluorescent protein ($\lambda_{ex}/\lambda_{em}$ = 540/570 nm). Imaging experiments were performed at DIV 14 when cortical neurons expressed a subset of NMDARs similar to those observed in adults. When transfected with cDNA encoding for DS-red, neurons displayed a cytosolic expression of the fluorescent protein that allowed the visualization of the dendritic morphology (Figure 3A). After exposure to fluorescent ligand **6**, a

punctate green fluorescence was demonstrable (Figure 3B). The merged image showed the yellow coloration that
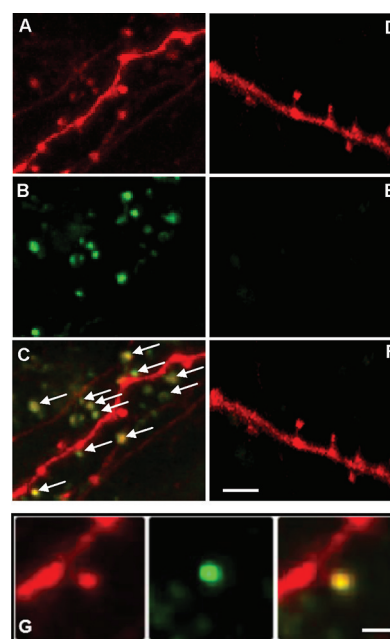
Figure 3. Confocal microscopy imaging. (A) Dendrite of Ds-red transfected cortical neurons (red, emission band 550−590 nm), (B) after 15 min exposition to 10 μM conjugate **6** (green, emission band 513−530 nm), (C) merge showing fluorescent yellow colocalization with dendritic spines (arrows). (D, E, F) Preincubation with ifenprodil **1** (15 min, 10 μM) fully blocked the probe **6** labeling. Scale bar 5 μm. (G) High magnification of a dendritic spine after 15 min exposition to 10 μM probe as in A, B, and C. Scale bar 1 μm.

characterizes the exact colocalization of red and green fluorescence, especially on small protrusions along the dendrites that could correspond to postsynaptic sites (Figure 3C). A high magnification of a spine labeled with probe **6** proved the localization of the staining on the protrusions (Figure 3G). To assess the specificity of the labeling, exposure with probe **6** was preceded by a preincubation with ifenprodil **1** (10 μM). Under these conditions, image acquisition with the same amplification setting failed to reveal any green fluorescence (Figure 3D−F). Inhibition of probe **6** staining by ifenprodil **1** strongly suggests that the fluorescent image in Figure 3B is due to a specific binding of probe **6** on NR2B-containing NMDARs.

In conclusion, we have reported here the synthesis of novel fluorescent ligands of NR2B-containing receptors on the basis of the structural framework of ifenprodil and of its original ethylenediamine analogue **10**. The derivative **10** was assayed for its ability to be recognized by the ifenprodil binding site, and to

retain NR2B selectivity. Ligand **10** was found to exhibit a potent inhibition of NR2B-containing receptors, partly through a mechanism of blockade at the channel pore. Fluorophore conjugation to ligand **10** led to fluorescent probes **4**, **6**, and **7** that displayed a moderate affinity for the NR2B subunit. Confocal microscopy imaging of DS-red labeled cortical neurons using the fluorescein conjugate **6** showed an exact colocalization of the probe with small protrusions along the dendrites which would highly support specific binding to NR2B-containing NMDARs. This unprecedented result demonstrates the proof-of-concept for NR2B-containing NMDAR imaging through the use of a selective, synthetic fluorescent ligand. The dense labeling of the dendritic spines, given the current resolution of our images, did not allow us to distinguish between an eventual synaptic and extrasynaptic localization, which will be the object of future investigations. Work is now in progress to develop novel generations of fluorescent probes with improved pharmacological profiles for further characterization, neuronal location, and biodistribution studies of NMDARs. These approaches would potentially open a wide field of applications in the pathophysiology of the central nervous system.

■ EXPERIMENTAL SECTION

HEK293 Cell Culture and Plasmid Transfection. CDNAs encoding the full length sequences of NR1−1a, NR2B-GFP, and NR2A-GFP were a generous gift from Dr. Stefano Vicini (Georgetown University Medical Center, Washington). Human embryonic kidney 293 cells (HEK 293) were grown in Dulbecco's medium (Invitrogen, France) supplemented with 1% L-glutamine, 1% streptomycin/penicillin/neomycin (Sigma-Aldrich), and 10% fetal bovine serum (Invitrogen). HEK cells were plated on 12 mm glass coverslips (MatTek Corporation, USA) coated with poly(D-lysine) and grown at 37 °C in a humidified atmosphere containing 5% CO_2. Twenty-four hours after plating, cells were transfected with cDNA encoding for NR1−1a/NR2A-GFP or NR2B-GFP using Transfast Reagent (Promega, France). After the transfection, HEK cells were cultured with an NMDA antagonist (D-APV at 100 μM) to prevent cell death.

Calcium Imaging. HEK 293 expressing NR1−1a/NR2B-GFP or NR1−1a/NR2A-GFP were loaded for 45 min at 37 °C with 10 μM Fura-2/AM and 0.2% pluronic acid (F-127, Invitrogen) and incubated for an additional 15 min at room temperature (rt) in HEPES and bicarbonate-buffered saline solution (HBBSS) containing (in mM) 116 NaCl; 5.4 KCl; 1.8 $CaCl_2$; 0.8 $MgSO_4$; 1.3 NaH_2PO_4; 12 HEPES; 5.5 glucose; 25 bicarbonate; and 10 μM glycine at pH 7.45. Experiments were performed at rt with continuous perfusion (at 2 mL/min) on the stage of a Nikon Eclipse inverted microscope equipped with a 100 W mercury lamp and oil immersion Nikon 40× objective with a 1.4 numerical aperture. Fura-2 (excitation: 340/380 nm, emission: 510 nm) ratio images were acquired every 2 s with a digital camera (Princeton Instruments, New Jersey, USA). Analysis was performed with the software *Metafluor 6.3* (Universal Imaging Corporation, New Jersey, USA). Measurements were carried out with amplification rates that prevented saturation of the fluorescence signal. Fluorescence ratios (340/380 nm) were converted to intracellular Ca^{2+} concentrations using the following formula:

$$[Ca^{2+}]_i = Kd[(R - R_{min})/(R_{max} - R)]F_0/F_s$$

where R is the ratio for observed 340/380 fluorescence ratio, R_{min} is a ratio for a Ca^{2+}-free solution, R_{max} is the ratio for a

saturated Ca^{2+} solution, K_d = 135 nM (the dissociation constant for Fura-2), F_0 is the intensity of a Ca^{2+}-free solution at 380 nm, and F_s is the intensity of a saturated Ca^{2+} solution at 380 nm. NMDA solutions (at 100 μM) were applied for 30 s, each application was separated by a minimum of 5 min to allow the full recovery to the basal level of $[Ca^{2+}]_i$. Ifenprodil **1** (purchased from Tocris) was used in its tartaric ammonium form whereas ligand **10** was used as hydrochloride ammonium. Fluorescent tracers **4**−**7** were used as obtained after lyophilization. Ligands were prepared as 1 mL aliquots at 10 mM in water for **1**, **7**, and **10**, and in DMSO for **4**−**6**. Because the slow rate of inhibition of ifenprodil,[36] ligands **1**, **4**−**7**, and **10** were applied 60 s prior to and during NMDA application. For each experiment, ROIs (Region Of Interest) corresponding to the cell bodies were chosen. The obtained fluorescence values were plotted against time to generate graphics of the intracellular Ca^{2+} trend in response to stimulation by NMDA (100 μM) in the presence of glycine (10 μM) and to ligand administration. To calculate the percentage of inhibition induced by the compounds of interest, we measured the $[Ca^{2+}]$ signal by integrating the area under the curve (AUC) on a 2 min period after the beginning of NMDA application. Dose−response curves were analyzed on the standard slope with *GraphPad Prism 5.0*.

Electrophysiology. Recombinant NMDA receptors were expressed in *Xenopus laevis* oocytes and currents measured using the two-electrode voltage-clamp technique. Oocyte preparation, injection, and superfusion were carried out as previously reported in the literature.[28] The extracellular medium contained (in mM) 100 NaCl, 2.5 KCl, 0.3 $BaCl_2$, 5 HEPES, and 0.01 diethylenetriamine-pentaacetic acid (DTPA; to chelate trace amount of heavy metals). The pH was adjusted to 7.3. All experiments were performed at rt. Dose−response curves were analyzed by the variable Hill slope with *GraphPad Prism 5.0*.

Confocal Imaging. To analyze the binding properties of the fluorescent ligand, we performed a spatial analysis of the fluorescent signal on murine primary cortical neuron cultures (at DIV 10), transfected with Ds-Red fluorescent protein ($\lambda_{ex}/\lambda_{em}$ = 540/570 nm). Transfections were performed with the phosphate-calcium technique. Neurons were exposed to cDNA for 2 h, and returned to DMEM. Experiments were performed at DIV 14 when the primary culture of murine cortical neurons expressed a subset of NMDA receptors similar to those expressed in adults (data not shown). Neurons were exposed to the fluorescent conjugate **6** (10 μM in DMSO/HBBSS 1:9, $\lambda_{ex}/\lambda_{em}$ = 490/525 nm) for 15 min and then washed with 5 mL of HBBSS. Images were acquired with Nikon EZ-C1 software at a resolution of 1024 × 1024 pixels. Sections of 0.3 μm were acquired in a Z-stack from top to bottom of the specimen. Specific fluorescence signal yield by the probe **6** was evaluated by the intensity obtained with the same laser power and gain intensity in each set of experiments.

■ ASSOCIATED CONTENT

Ⓢ Supporting Information

Full synthetic procedures, analytical and spectral characterization data of the synthesized compounds. This material is available free of charge via the Internet at http://pubs.acs.org.

■ AUTHOR INFORMATION

Corresponding Author

*Phone: (33)231470281. Fax: (33)231470275. E-mail: perrio@ cyceron.fr.

■ REFERENCES

(1) Brauner-Osborne, H., Egebjerg, J., Nielsen, E. O., Madsen, U., and Krogsgaard-Larsen, P. (2000) Ligands for glutamate receptors: design and therapeutic prospects. *J. Med. Chem. 43*, 2609−2645.

(2) Paoletti, P., and Neyton, J. (2007) NMDA receptor subunits: function and pharmacology. *Curr. Opin. Pharmacol. 7*, 39−47.

(3) Chazot, P. L. (2004) The NMDA receptor NR2B subunit: a valid therapeutic target for multiple CNS pathologies. *Curr. Med. Chem. 11*, 389−396.

(4) Childers, W. E. Jr., and Baudy, R. B. (2007) N-Methyl-D-aspartate antagonists and neuropathic pain: the search for relief. *J. Med. Chem. 50*, 2557−2562.

(5) Higgins, G. A., Ballard, T. M., Enderlin, M., Haman, M., and Kemp, J. A. (2005) Evidence for improved performance in cognitive tasks following selective NR2B NMDA receptor antagonist pre-treatment in the rat. *Psychopharmacology 179*, 85−98.

(6) Gogas, K. R. (2006) Glutamate-based therapeutic approaches: NR2B receptor antagonists. *Curr. Opin. Pharmacol. 6*, 68−74.

(7) Laube, B., Kuhse, J., and Betz, H. (1998) Evidence for a tetrameric structure of recombinant NMDA receptors. *J. Neurosci. 18*, 2954−2961.

(8) Loftis, J. M., and Janowsky, A. (2003) The N-methyl-D-aspartate receptor subunit NR2B: localization, functional properties, regulation, and clinical implications. *Pharmacol. Therapeutics 97*, 55−85.

(9) Paoletti, P. (2011) Molecular basis of NMDA receptor functional diversity. *Eur. J. Neurosci. 33*, 1351−1365.

(10) Cull-Candy, S. G., and Leszkiewicz, D. N. (2004) Role of distinct NMDA receptor subtypes at central synapses. *Sci. STKE 255*, re16.

(11) Hardingham, G. E., Fukunaga, Y., and Bading, H. (2002) Extra-synaptic NMDARs oppose synaptic NMDARs by triggering CREB shut-off and cell death pathways. *Nat. Neurosci. 5*, 405−414.

(12) Mony, L., Kew, J. N. C., Gunthorpe, M. J., and Paoletti, P. (2009) Allosteric modulators of NR2B-containing NMDA receptors: molecular mechanisms and therapeutic potential. *Br. J. Pharmacol. 157*, 1301−1317.

(13) McGrath, J. C., Arribas, S., and Daly, C. J. (1996) Fluorescent ligands for the study of receptors. *Trends Pharmacol. Sci. 17*, 393−399.

(14) Reynold, I. J., and Miller, R. (1989) Ifenprodil is a novel type of N-methyl-D-aspartate receptor antagonist: interaction with polyamines. *Mol. Pharmacol. 36*, 758−765.

(15) Chenard, B. L., Shalaby, I. A., Koe, B. K., Ronau, R. T., Butler, T. W., Prochniak, M. A., Schmidt, A. W., and Fox, C. B. (1991) Separation of α_1-adrenergic and N-methyl-D-aspartate antagonist activity in a series of ifenprodil compounds. *J. Med. Chem. 34*, 3085−3090.

(16) Williams, K. (2001) Ifenprodil, a novel NMDA receptor antagonist: site and mechanism of action. *Curr. Drug Targets 2*, 285−298.

(17) Borza, I., and Domany, G. (2006) NR2B selective NMDA antagonists: the evolution of the ifenprodil-type pharmacophore. *Curr. Top. Med. Chem. 6*, 687−695.

(18) Layton, M. E., Kelly, M. J. III, and Rodzinak, K. J. (2006) Recent advances in the development of NR2B subtype-selective NMDA receptor antagonists. *Curr. Top. Med. Chem. 6*, 697−709.

(19) MacCauley, J. A. (2006) Amide-containing NR2B/NMDA receptor antagonists. *Expert Opin. Ther. Patents 16*, 863−870.

(20) MacCauley, J. A. (2005) NR2B subtype-selective NMDA receptor antagonists: 2001−2004. *Expert Opin. Ther. Patents 15*, 389−407.

(21) Nikam, S. S., and Meltzer, L. T. (2002) NR2B selective NMDA receptor antagonists. *Curr. Pharm. Des. 8*, 845−855.

(22) Rosahl, T. W., Wingrove, P. B., Hunt, V., Fradley, R. L., Lawrence, J. M. K., Heavens, R. P., Treacey, P., Usala, M., Macauley, A., Bonnert, T. P., Whiting, P. J., and Wafford, K. A. (2006) A genetically modified mouse model probing the selective action of ifenprodil at the N-methyl-D-aspartate type 2B receptor. *Mol. Cell. Neurosci. 33*, 47−56.

(23) Grimwood, S., Richards, P., Murray, F., Harrison, N., Wingrove, P. B., and Hutson, P. H. (2000) Characterisation of N-methyl-D-aspartate receptor-specific [3H]ifenprodil binding to recombinant human NR1a/NR2B receptors compared with native receptors in rodent brain membranes. *J. Neurochem. 75*, 2455−2463.

(24) Avenet, P., Leonardon, J., Besnard, F., Graham, D., Frost, J., Depoortere, H., Langer, S. Z., and Scatton, B. (1996) Antagonist properties of the stereoisomers of ifenprodil at NR1A/NR2A and NR1A/NR2B subtypes of the NMDA receptor expressed in Xenopus oocytes. *Eur. J. Pharmacol. 296*, 209−213.

(25) Tamiz, A. P., Whittemore, E. R., Zhou, Z.-L., Huang, J.-C., Drewe, J. A., Chen, J.-C., Cai, S.-X., Weber, E., Woodward, R. M., and Keana, J. F. W. (1998) Structure-activity relationships for a series of bis(phenylalkyl)amines: potent subtype-selective inhibitors of N-methyl-D-aspartate receptors. *J. Med. Chem. 41*, 3499−3506.

(26) Masuko, T., Kashiwagi, K., Kuno, T., Nguyen, N. D., Pahk, A. J., Fukuchi, J., Igarashi, K., and Williams, K. (1999) A regulatory domain (R1-R2) in the amino terminus of the N-methyl-D-aspartate receptor: effects of spermine, protons, and ifenprodil, and structural similarity to bacterial leucine/isoleucine/valine binding protein. *Mol. Pharmacol. 55*, 957−969.

(27) Perin-Dureau, F., Rachline, J., Neyton, J., and Paoletti, P. (2002) Mapping the binding site of the neuroprotectant ifenprodil on NMDA receptors. *J. Neurosci. 22*, 5955−5965.

(28) Mony, L., Krzaczkowski, L., Leonetti, M., Le Goff, A., Alarcon, K., Neyton, J., Bertrand, H.-O., Acher, F., and Paoletti, P. (2009) Structural basis of NR2B-selective antagonist recognition by N-methyl-D-aspartate receptors. *Mol. Pharmacol. 75*, 60−74.

(29) Ng, F.-M., Geballe, M. T., Snyder, J. P., Traynelis, S. F., and Low, C.-M. (2008) Structural insights into phenylethanolamines high-affinity binding site in NR2B from binding and molecular modeling studies. *Molecular Brain 1* (16), 1−11.

(30) MacCauley, J. A., Theberge, C. R., Romano, J. J., Billings, S. B., Anderson, K. D., Claremon, D. A., Freidinger, R. M., Bednar, R. A., Mosser, S. D., Gaul, S. L., Connolly, T. M., Condra, C. L., Xia, M., Cunningham, M. E., Bednar, B., Stump, G. L., Lynch, J. J., Macaulay, A., Wafford, K. A., Koblan, K. S., and Liverton, N. J. (2004) NR2B-Selective N-methyl-D-aspartate antagonists: synthesis and evaluation of 5-substituted benzimidazoles. *J. Med. Chem. 47*, 2089−2096.

(31) Saravanan, P., Bisai, A., Baktharaman, S., Chandrasekhar, M., and Singh, V. K. (2002) Synthesis of chiral non-racemic 1,2-diamines from O-acetyl mandelic acid: application in enantioselective deprotonation of epoxides and diethylzinc addition to aldehydes. *Tetrahedron 58*, 4693−4706.

(32) Dingledine, R., Borges, K., Bowie, D., and Traynelis, S. F. (1999) The glutamate receptor ion channels. *Pharmacol. Rev. 51*, 7−61.

(33) Yuan, H., Hansen, K. B., Vance, K. M., Ogden, K. K., and Traynelis, S. F. (2009) Control of NMDA receptor function by the NR2 subunit amino-terminal domain. *J. Neurosci. 29*, 12045−12058.

(34) For example: Rock, D. M., and MacDonald, R. L. (1992) The polyamine spermine has multiple actions on N-methyl-D-aspartate receptor single-channel currents in cultured cortical neurons. *Mol. Pharmacol. 41*, 83−88.

(35) Han, X., Tomitori, H., Mizuno, S., Higashi, K., Füll, C., Fukiwake, T., Terui, Y., Leewanich, P., Nishimura, K., Toida, T., Williams, K., Kashiwagi, K., and Igarashi, K. (2008) Binding of spermine and ifenprodil to a purified, soluble regulatory domain of the N-methyl-D-aspartate receptor. *J. Neurochem. 107*, 1566−1577.

(36) Williams, K. (1993) Ifenprodil discriminates subtypes of the N-methyl-D-aspartate receptor: selectivity and mechanisms at recombinant heteromeric receptors. *Mol. Pharmacol. 44*, 851−859.